ANALYSIS OF A MULTIPLICATIVE HYBRID ROUTE CHOICE MODEL IN STOCHASTIC ASSIGNMENT PARADOX

Zhanhong Cheng[1], Jia Yao[1, 2*], Anthony Chen[3], Shi An[1]

ABSTRACT

In recent years, a multiplicative hybrid (MH) route choice model was proposed to overcome the drawbacks of the multinomial logit (MNL) model and the multinomial weibit (MNW) model. This paper compares the conditions for the stochastic traffic assignment paradox of the three models. We analyze the condition when improving a link in an uncongested network counterintuitively increases total travel costs. Using three typical flow-independent networks (two links, n independent links, and n routes with m overlapping links), we reveal the strong relationships in the paradox conditions of the three models. We further study the paradoxical features of the three models in the Sioux-Falls network, where the model parameters are estimated from simulated route sets. The case study shows that 1) the MH model fits the data the best, 2) using the MNL or the MNW model to identify paradox links exhibits intrinsic tendencies that are consistent with the theoretical analysis, and 3) the paradox links identified by the MH model is a compromise of the other two models. This paper delves into the relationships of the three models in the stochastic assignment paradox and provides suggestions and caveats to the application of the three models.

Keywords: transportation; traffic paradox; route choice; stochastic traffic assignment; paradox condition

[1] School of Transportation Science and Engineering, Harbin Institute of Technology, Harbin, Heilongjiang 150090, P. R. China

[2] School of Economics and Management, Dalian University of Technology, Dalian, Liaoning 116024, P. R. China

[3] Department of Civil and Environmental Engineering, The Hong Kong Polytechnic University, Hunghom, Hong Kong

[*] Corresponding author. E-mail address: yaojia@hit.edu.cn (J. Yao)

1. Introduction

The history of the traffic paradox can be traced back to 1968 when Braess discovered that adding a new link to a congested network may increase overall travel costs (Braess, 1968; Braess et al., 2005). The occurrence of this phenomenon owes to the discrepancy between user equilibrium condition (Wardrop, 1952) and system optimal flow assignment.

The traffic paradox has received considerable attention for its both theoretical and practical significance. In traffic network planning, it is particularly hard to evaluate the effect of a plan beforehand. From a personal level, travelers often fail to unite as a whole to maximize the network's utility. Sometimes, a well-intentioned improvement may aggravate network-wide congestion. In the literature, the Braess paradox has been studied under different circumstances, including Braess paradox under elastic demand assignment (Hallefjord et al., 1994; Yang, 1997), dynamic assignment (Arnott et al., 1993; Akamatsu, 2000; Zhang et al., 2008; Lin and Lo, 2009), stochastic equilibrium (Prashker and Bekhor, 2000; Zhao et al., 2014), combined distribution and assignment (Zhou et al., 2009; Yang and Chen, 2009), boundedly rational user equilibrium (Di et al., 2014). Methods are developed to detect the "paradox roads" in the real network (Sun et al., 2015; Bagloee et al., 2017; Ma et al., 2018), and the Braess paradox has even been observed in air networks (Ma et al., 2019). On the other hand, other paradoxes have been studied, such as Downs-Thomson paradox (Downs, 1962; Thomson, 1978; Wang et al., 2017), stochastic assignment paradox (Sheffi and Daganzo, 1978; Yao and Chen, 2014), capacity paradox (Yang and Bell, 1998), emission paradox (Nagurney, 2000; Szeto et al., 2008), reliability paradox (Szeto, 2011), transit assignment (Szeto and Jiang, 2014), exclusive bus lanes' setting paradox (Yao et al., 2015), traffic noise paradox (Wang and Szeto, 2017), and information Braess paradox (Acemoglu et al., 2018; Yao et al., 2019a).

This paper focuses on the stochastic assignment paradox (Sheffi and Daganzo, 1978) in uncongested networks where "too many" travelers shift to an improved facility even though it is still an inferior alternative. The stochastic assignment paradox is caused by travelers' perception error, and it performs differently under different stochastic route choice models (Henn and Ottomanelli, 2006). The most widely used route choice model is the multinomial logit (MNL) model, which is developed early and has a closed-form probability expression. Castillo et al. (2008) proposed another closed-form route choice model, the multinomial weibit (MNW) model. Although with the closed forms, both the MNL and MNW models have obvious drawbacks. Because of the assumption that random error terms are independently and identically distributed (IID) Gumbel variates, the MNL model can account for neither overlapping (or correlation) among routes nor perception variance with respect to trips of different lengths (Sheffi, 1985). For the MNW model, the identically distributed assumption is not required, and the random error term is subject to an independently Weibull distribution. Although MNW model can identify different trip lengths by different perception variances (Castillo et al., 2008), it also has its limitation of not being able to identify any arbitrary multiplier on the route cost (Kitthamkesorn and Chen, 2014). Therefore, Xu et al. (2015) proposed a multiplicative hybrid (MH) model that alleviates the drawbacks of both MNL and MNW models. The hybrid model keeps the closed-form probability expression and is very suitable for practical applications. For example, Liu et al. (2017) proposed a select link analysis method based on the MH model.

It is very important to understanding the conditions that produce traffic paradoxes (Yao and Chen, 2014; Yao et al., 2019b; Kitahara and Hayakawa, 2019). The conditions of the stochastic assignment paradox for the MNL model and the MNW model were analyzed by Yao and Chen (2014); results showed the stochastic assignment paradox depends on how the cost difference is considered in the route choice model. Based on

their study, this paper tries to connect the MH model with the original two models (i.e., MNL and MNW) by investigating their stochastic assignment paradox when an inferior travel alternative is marginally improved. Based on the theoretical analysis, we further demonstrate some intrinsic tendencies when using the three models in identifying paradox links in the Sioux-Falls Network. This paper reveals some theoretical properties of using the three models for stochastic assignment paradox identification and therefore could better support decision making.

The remainder of this paper is organized as follows. Section 2 briefly introduces the MH model and its alleviation in the drawbacks of the MNL and MNW models. In Section 3, paradoxical features of the MH model are analyzed in three typical networks: (1) a two-link network; (2) a single O-D pair's network with n independent links; (3) a n route single O-D pair's network with m overlapping links. Section 4 compares the stochastic paradox of the three models when using the estimated parameters. Conclusions and further research are summarized in the last section.

2. A brief review of the hybrid model

The multiplicative hybrid (MH) model proposed by Xu et al. (2015) combines the MNL model and the MNW model. For the MH model, the route choice probability of route k in O-D pair i is

$$p_k^i = \frac{\exp\left(-\theta c_k^i\right) {c_k^i}^{-\beta}}{\sum_{l \in K^i} \exp\left(-\theta c_l^i\right) {c_l^i}^{-\beta}} = \frac{1}{\sum_{l \in K^i} \exp\left(-\theta (c_l^i - c_k^i)\right) \left(\frac{c_l^i}{c_k^i}\right)^{-\beta}}; \quad \forall\ k \in K^i,\ i \in I\ . \tag{1}$$

where I is the set of O-D pairs, K^i is the route set within the O–D pair i, c_k^i is the cost of route k of O-D pair i, θ is the dispersion parameter of Gumbel random error distribution, and β is the shape parameter of the Weibull random error distribution. Like in the original MNL and MNW models, θ and β are related to the variance of the stochastic perceived error. The larger the θ and the β, the smaller the perception error, and the smaller the probability to choose non-shortest paths. Note that Eq. (1) contains both absolute cost difference (i.e., $c_l^i - c_k^i$) and relative cost difference (i.e., c_l^i / c_k^i); this alleviates the drawbacks of both the MNL and MNW models.

A two-link network shown in Fig. 1 is used to demonstrate the superiority of the MH model. In Fig. 1, c_1 is the travel cost of the upper route (route 1) and c_2 is the travel cost of the lower route (route 2).

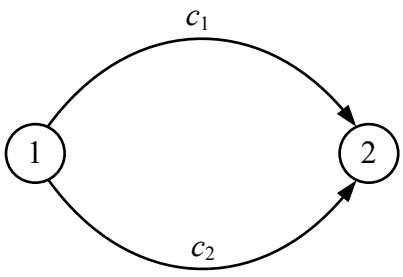

Fig. 1. Network I: Single O-D pair's network with two links.

Let $\theta = 0.1$, $\beta = 3$. When $c_2 = c_1 + 5$ (constant absolute difference), the probabilities of the three models to choose route 1 with different c_1 are shown in Fig. 2 (a). Correspondingly, the probabilities when $c_2 =$

$2c_1$ (constant relative difference) are shown in Fig. 2 (b). Fig. 2 (a) shows that p_1 of the MNL model is unchanged with different c_1 under constant absolute route costs difference; Fig. 2 (b) shows that p_1 of the MNW model is unchanged with different c_1 under constant relative difference. The MNL/MNW model fails to distinguish the situations with constant absolute/relative costs difference. Both are counter intuitive. The MH model, however, overcomes the drawback of the original two models and is sensitive to both absolute and relative differences.

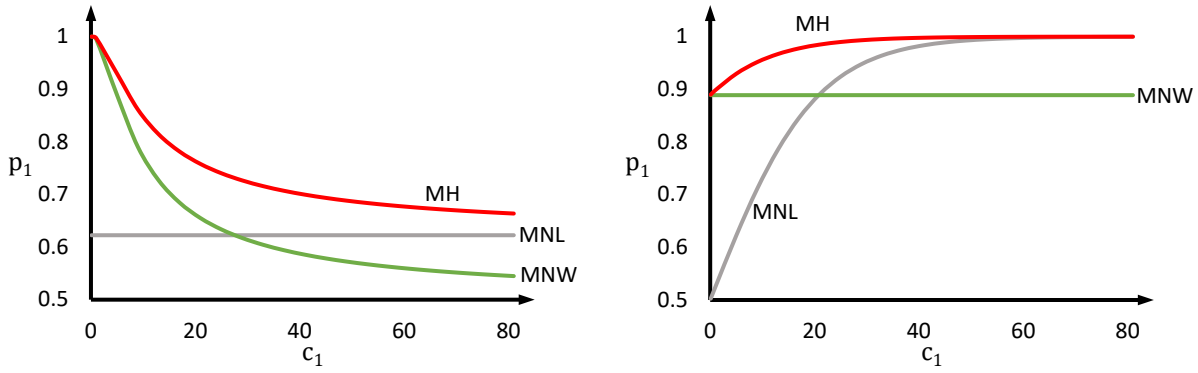

(a) $c_2 = c_1 + 5$ (b) $c_2 = 2c_1$

Fig. 2. Different route choice features of the three route choice models.

Look at the MH model from another perspective, Eq. (1) can be transformed to

$$p_k^i = \frac{\exp\left(-\theta c_k^i - \beta \ln c_k^i\right)}{\sum_{l \in K^i} \exp\left(-\theta c_l^i - \beta \ln c_l^i\right)}; \quad \forall\ k \in K^i,\ i \in I. \tag{2}$$

Eq. (2) is similar to the MNL model but with a different utility term. The utility of a route should not increase with the increase of its costs, which suggests that $\theta \geq 0$ and $\beta \geq 0$ must hold in the MNL model and the MNW model. For the MH model, there should be

$$\frac{\partial\left(-\theta c_k^i - \beta \ln c_k^i\right)}{\partial c_k^i} = -\theta - \frac{\beta}{c_k^i} \leq 0; \quad \forall\ k \in K^i,\ i \in I. \tag{3}$$

Theoretically, the cost of a route c_k^i can be any positive real number. Therefore, θ and β should be non-negative to guarantee the Eq. (3) always holds.

3. Stochastic assignment paradox of the hybrid model

In a stochastic traffic assignment paradox, we focus on the condition when marginally improving a link (i.e., reducing the link cost) increases the total network travel cost. The "marginal" means the reduction of the link's cost approaches zero. In other words, the total network travel cost, in the vicinity, is a decreasing function of the link cost. In this section, the stochastic assignment paradox of the MH model is studied under three representative cases: (1) the two-link network shown in Fig. 1; (2) a single O-D pair's network with n independent links; (2) a single O-D pair's network with one overlapping link.

3.1. Two-link network

For the two-link network shown in Fig. 1, the total travel cost of the MH model is:

$$C^{MH} = Q(c_1 p_1 + c_2 p_2) = Q\left(\frac{c_1 \exp(-\theta c_1){c_1}^{-\beta} + c_2 \exp(-\theta c_2){c_2}^{-\beta}}{\exp(-\theta c_1){c_1}^{-\beta} + \exp(-\theta c_2){c_2}^{-\beta}}\right), \tag{4}$$

where Q is the O-D demand. To analyze the effect of the marginal improvement of route 1 on the total travel cost C^{MH}, the partial derivative of C^{MH} with respect to c_1 is derived as follows:

$$\frac{\partial C^{MH}}{\partial c_1} = Q\frac{MH(c_1,c_2)}{\exp(\theta(c_1+c_2))(c_1c_2)^{\beta}\left(\exp(-\theta c_1){c_1}^{-\beta} + \exp(-\theta c_2){c_2}^{-\beta}\right)^2}, \tag{5}$$

where

$$MH(c_1,c_2) = \exp\big(\theta(c_2-c_1)\big)\left(\frac{c_2}{c_1}\right)^{\beta} + \beta\left(\frac{c_2}{c_1}\right) + \theta(c_2-c_1) + 1 - \beta. \tag{6}$$

$\partial C^{MH}/\partial c_1 < 0$ describes a circumstance where the marginal decrease in the cost of route 1 results in an increase in the total travel cost, which means the traffic paradox occurs. And $\partial C^{MH}/\partial c_1 > 0$ indicates paradox does not occur. For convenience, the circumstance where $\partial C^{MH}/\partial c_1 = 0$ is referred to as the paradox boundary. Clearly, the sign of $\partial C^{MH}/\partial c_1$ is only determined by $MH(c_1,c_2)$.

It is hard to analytically derive the expression of the paradox boundary of the MH model because of the complex expression of $MH(c_1,c_2)$. However, it is possible to analyze the relations between the paradox boundary of the MH model and the original two models. The partial derivative of the total travel cost with respect to c_1 in the MNL model and the MNW model are

$$\frac{\partial C^{L}}{\partial c_1} = Q\frac{L(c_1,c_2)}{\exp(\theta(c_2+c_1))(\exp(-\theta c_1)+\exp(-\theta c_2))^2} \tag{7}$$

and

$$\frac{\partial C^{W}}{\partial c_1} = Q\frac{W(c_1,c_2)}{(c_1c_2)^{\beta}\left({c_1}^{-\beta}+{c_2}^{-\beta}\right)^2} \tag{8}$$

respectively, where

$$L(c_1,c_2) = \exp(\theta(c_2-c_1)) + \theta(c_2-c_1) + 1 \tag{9}$$

and

$$W(c_1,c_2) = (c_2/c_1)^{\beta} + \beta(c_2/c_1) + 1 - \beta. \tag{10}$$

Clearly, the signs of $\partial C^{L}/\partial c_1$ and $\partial C^{W}/\partial c_1$ are determined by $L(c_1,c_2)$ and $W(c_1,c_2)$. As discussed by Yao and Chen (2014), the paradox boundaries of the MNL model and the MNW model exhibit a linear trend. The paradox boundary of the MNL model is related to the absolute cost difference of the two routes, satisfying $c_1 = c_2 + 1.28/\theta$. The paradox boundary of the MNW model is related to the relative cost difference of the two routes, satisfying $c_1 = c_2/x_0(\beta)$, where $x_0(\beta) \in (0,1)$ is the root of the function $W(x|\beta) = x^{\beta} + \beta x + 1 - \beta$ (refer to Yao and Chen (2014) for details).

Note that the paradox of the MNW model does not exist in the two-link network when $0 < \beta \leq 1$. And we will discuss the paradox boundary of the MH model under two circumstances: 1) when $\beta > 1$ and 2) when $0 < \beta \leq 1$.

3.1.1. When $\beta > 1$

We first visually examine the three models' paradox boundaries under $\theta = 0.1$ and $\beta = 3$. Given a fixed c_2, the corresponding c_1 on a paradox boundary can be numerically solved by finding the root when the derivative is zero (i.e., when Eq. (6), Eq. (9), or Eq. (10) equals zero). Given a sequence of c_2, the paradox boundaries of the three models, in two different coordinate systems, are obtained numerically and shown in Fig. 3 (Note that the axes of c_1 and c_2 in Fig. 3 (a) are exchanged compared with the work of Yao and Chen (2014) for the consistency with section 3.2). The paradox boundary of each model distinguishes the area whether marginally improving c_1 brings a paradox.

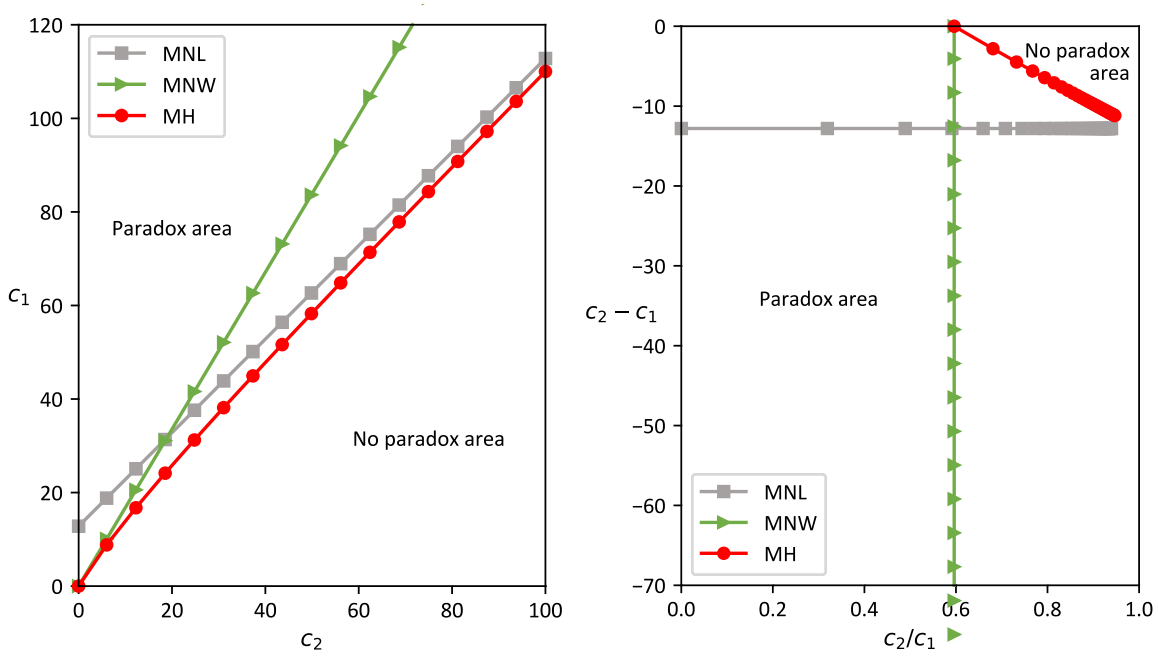

(a) c_2 and c_1 coordinate system (b) c_2/c_1 and $c_2 - c_1$ coordinate system

Fig. 3 Paradox area of the MNL, MNW and MH models when $\theta = 0.1$ and $\beta = 3$

For the MH model, note that:

$$\frac{\partial MH(c_1,c_2)}{\partial c_1} = -\left(\exp\left(\theta(c_2 - c_1)\right)\left(\frac{c_2}{c_1}\right)^{\beta}\left(\theta + \frac{\beta}{c_1}\right) + \theta + \frac{\beta c_2}{c_1^2}\right) < 0. \tag{11}$$

Therefore, $MH(c_1, c_2)$ is a monotonically decreasing function with respect to c_1. And the area above the paradox boundary in Fig. 3 (a) satisfies $MH(c_1, c_2) < 0$, which represents the paradox area of the MH model. Further, the following observations of the MH model can be obtained from Fig. 3.

1. Intuitively, the paradox boundary of the MH model in Fig. 3 (a) is not linear. It starts from the origin, and when $c_2 \to 0^+$, the MH model has a same paradox feature with the MNW model.

2. In Fig. 3 (a), when c_2 gets bigger, there is a trend that the paradox boundary of the MH model will approximate to the paradox boundary of the MNL model.

3. The MH model has a larger paradox area than the other two models and the paradox boundary of the MH

model in Fig. 3 (a) is lower than both the curves of the MNL and MNW models.

The observations listed above show the key paradoxical features of the MH model as well as its connections with the two original models. Moreover, these features can be formally written into propositions and rigorously proved. Propositions and proofs are displayed as follows in the order of its corresponding observations listed above.

Proposition 1. For any $\theta \in (0,+\infty)$, $\beta \in (1,+\infty)$, when $c_2 \to 0^+$, the root of $MH(c_1,c_2)=0$ approaches to the root of $W(c_1,c_2)=0$.

Proof. When $W(c_1,c_2)=0$, there is $c_1 = c_2/x_0(\beta)$; $x_0(\beta) \in (0,1)$.

When $c_2 \to 0^+$,

$$c_2 - c_1 = c_2\left(1 - 1/\ x_0(\beta)\right) \to 0, \tag{12}$$

Thus,

$$MH(c_1,c_2) \to \left(\frac{c_2}{c_1}\right)^{\beta} + \beta\left(\frac{c_2}{c_1}\right) + 1 - \beta = \mathrm{W}(c_1,c_2). \tag{13}$$

Therefore, when $c_1 \to 0^+$, the root of $MH(c_1,c_2)=0$ approaches to the root of $W(c_1,c_2)=0$. □

Proposition 2. For any $\theta \in (0,+\infty)$, $\beta \in (1,+\infty)$, when $c_2 \to +\infty$, the root of $MH(c_1,c_2)=0$ approaches to the root of $L(c_1,c_2)=0$.

Proof. When $L(c_1,c_2)=0$, there is $c_1 = c_2 + 1.28/\theta$.

When $c_2 \to +\infty$,

$$\frac{c_2}{c_1} = \frac{c_2}{c_2+\frac{1.28}{\theta}} = \frac{1}{1+\frac{1.28}{c_2\theta}} \to 1 \tag{14}$$

Thus,

$$MH(c_1,c_2) \to e^{\theta(c_2-c_1)} + \theta(c_2-c_1) + 1 = L(c_1,c_2). \tag{15}$$

Therefore, When $c_2 \to +\infty$, the root of $MH(c_1,c_2)=0$ approaches to the root of $L(c_1,c_2)=0$. □

Proposition 3. For any $\theta \in (0,+\infty)$, $\beta \in (1,+\infty)$, the paradox boundary of the MH model is always below the paradox boundary of the MNW model in Fig. 3(a).

Proof.

For any given $c_2 > 0$, $\theta \in (0,+\infty)$ and $\beta \in (1,+\infty)$, let the solution of $MH(c_1,c_2)=0$ to be $c_1 = mh(c_2)$ and the solution of $W(c_1,c_2)=0$ to be $c_1 = w(c_2)$. Then,

$$\begin{aligned} MH(w(c_2),c_2) &= MH(w(c_2),c_2) - W(w(c_2),c_2) \\ &= \left(e^{\theta(c_2-w(c_2))} - 1\right)\left(\frac{c_2}{w(c_2)}\right)^{\beta} + \theta(c_2 - w(c_2)). \end{aligned} \tag{16}$$

Since $w(c_2) = c_2/x_0(\beta)$, Eq.(16) can be rewritten as

$$MH(w(c_2), c_2) = \left(e^{\theta c_2(1-1/x_0(\beta))} - 1\right)x_0(\beta)^\beta + \theta c_2\left(1 - 1/x_0(\beta)\right). \quad (17)$$

For any $x_0(\beta) \in (0,1)$, $1 - 1/x_0(\beta) < 0$, then $e^{\theta c_2(1-1/x_0(\beta))} < 1$, thus $MH(w(c_2), c_2) < 0$. Then, $MH(hm(c_2), c_2) - MH(w(c_2), c_2) > 0$. According to Eq. (11), $MH(c_1, c_2)$ is a monotonically decreasing function with respect to c_1. Thus $mh(c_2) < w(c_2)$, which means the paradox boundary of the MH model is always below the paradox boundary of the MNW model in Fig. 3(a) for any $\theta \in (0, +\infty)$, $\beta \in (1, +\infty)$. □

Proposition 4. For any $\theta \in (0, +\infty)$, $\beta \in (1, +\infty)$, the paradox boundary of the MH model is always below the paradox boundary of the MNL model in Fig. 3(a).

Proof.

For any given $c_2 > 0$, $\theta \in (0, +\infty)$ and $\beta \in (1, +\infty)$, let the solution of $MH(c_1, c_2) = 0$ to be $c_1 = mh(c_2)$ and the solution of $L(c_1, c_2) = 0$ to be $c_1 = l(c_2)$. Then,

$$\begin{aligned} MH(l(c_2), c_2) &= MH(l(c_2), c_2) - L(l(c_2), c_2) \\ &= e^{\theta(c_2 - l(c_2))}\left(\frac{c_2}{l(c_2)}^\beta - 1\right) + \beta\left(\frac{c_2}{l(c_2)} - 1\right). \end{aligned} \quad (18)$$

Since $l(c_2) = c_2 + 1.28/\theta$, Eq.(18) can be rewritten as

$$MH(l(c_2), c_2) = e^{\theta(-1.28/\theta)}\left(\frac{c_2}{c_2 + 1.28/\theta}^\beta - 1\right) + \beta\left(\frac{c_2}{c_2 + 1.28/\theta} - 1\right). \quad (19)$$

When $\theta \in (0, +\infty)$, $\beta \in (1, +\infty)$, $\frac{c_2}{c_2 + 1.28/\theta}^\beta < 1$ and $\frac{c_2}{c_2 + 1.28/\theta} < 1$, thus $MH(l(c_2), c_2) < 0$. Then, $MH(hm(c_2), c_2) - MH(l(c_2), c_2) > 0$. According to Eq. (11), $MH(c_1, c_2)$ is a monotonically decreasing function with respect to c_1. Thus $mh(c_2) < l(c_2)$, which means that the paradox boundary of the MH model is always below the paradox boundary of the MNL model in Fig. 3(a) for any $\theta \in (0, +\infty)$, $\beta \in (1, +\infty)$. □

3.1.2. When $0 < \beta \leq 1$

When $0 < \beta \leq 1$, it is not hard to find that the Proposition 2 is still true. The paradox boundary of the MH model still approaches to the paradox boundary of the MNL model when $c_2 \to +\infty$. However, Proposition 1 is not true as there is no paradox for the MNW model under this condition. When $0 < \beta \leq 1$ and $c_2 \to 0^+$, let $c_1 = (1 - \beta)/\theta$, there is

$$MH(c_1, c_2) \to \exp\left(\theta(c_2 - c_1)\right) \times 0^\beta + \beta \times 0 + \theta\left(0 - \frac{1-\beta}{\theta}\right) + 1 - \beta = 0. \quad (20)$$

Therefore, the paradox boundary when $c_2 \to 0^+$ approaches to $(1 - \beta)/\theta$. Note that when $\beta = 1$ and $c_2 \to 0^+$, then $c_1 \to (1 - \beta)/\theta = 0$. This relates to the paradox boundary when $\beta \to 1^+$. Therefore, the paradox boundary of the MH changes continuously from $\beta = 1$ to $\beta = 1^+$.

However, the paradox boundary of the MH model does not change continuously from $\beta \to 0^+$ to $\beta = 0$. In fact, when $\beta \to 0^+$ and $c_2 \to 0^+$, the paradox boundary of the MH model is undeterminable. Because

$\lim_{c_2 \to 0^+, \beta \to 0^+} \left(\frac{c_2}{c_1}\right)^{\beta}$ is equivalent to $\lim_{x \to 0^+} x^x$, and this is mathematically undeterminable. While the MH model is equivalent to the MNL model when $\beta = 0$, there is a jump from $\beta \to 0^+$ to $\beta = 0$

3.1.3. Discussions about the parameters

According to the analysis above, for any fixed $\theta > 0$ and $\beta > 1$, the MH model always has a bigger paradox area than the MNL model and the MNW model. However, it does not mean that the MH model is more likely to encounter a paradox when applied in practice. When real data is used to estimate the value of β and θ, the estimated $\hat{\theta}$ and $\hat{\beta}$ in the MH model may be different from which in the MNL and MNW models. This section focuses on how the paradox boundary of the MH model changes if the MH model has different parameters with the MNL model and the MNW model, and the relations of the estimated parameters of the three models will be discussed in section 4.3.

Fig. 4 shows how the parameters' change affects the paradox area of the MH model. The original paradox boundary is shown in the solid line, and the dashed line represents the paradox boundary after the change. For comparison, three models are represented in different colors.

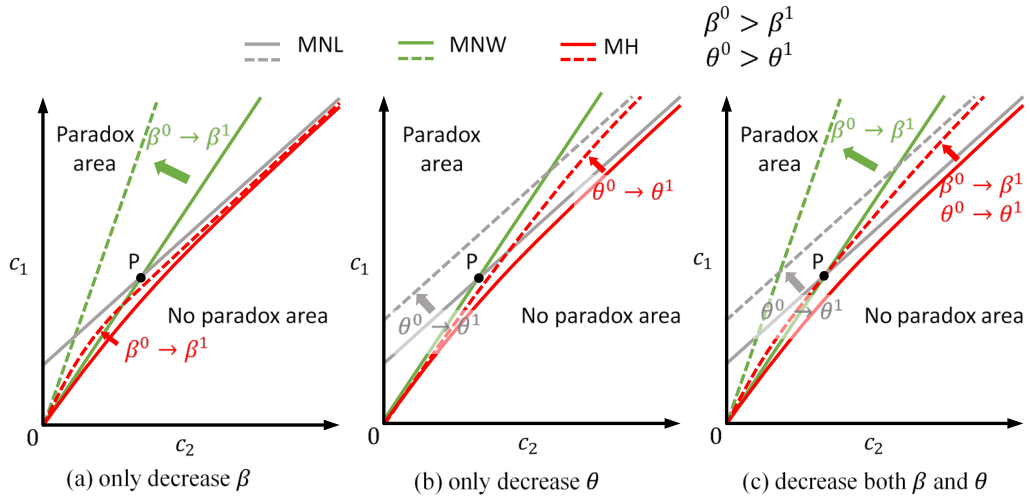

Fig. 4. Changes in paradox area of the MH model with respect to θ and β.

As is shown in Fig. 4(a), when β^0 decreases to β^1, the paradox boundary of the MNW model will move up and give a smaller paradox area. According to Proposition 1, in the near to zero area, the MH model's boundary will also shift up since it is dominated by MNW model. However, the up-shift of the curve of the MH model is limited by θ^0, Proposition 4 indicates that the paradox boundary of the MH model is always under the paradox boundary of the MNL model under the same θ. Therefore, the changed boundary of the MH model is still under the original MNL boundary; specifically, under the intersection point of the original boundaries of the MNL and MNW models (Point P).

Similarly, when only decreases θ, the new paradox boundaries of the MNL and MH models will shift up, but the up-shift of the curve of the MH model is limited by β^0, so the changed curve of the MH model is still under the original boundary of the MNL model as shown in Fig. 4(b).

When β and θ are decreased simultaneously, the changed MH model could be considered as a compromise

of the original MNL and MNW models as shown in Fig. 4(c).

3.2. Single O-D pair's network with n independent links

In the remaining part of section 3, the discussion is confined on the cases when $\theta > 0$ and $\beta > 1$ as there is no paradox for either the MNL model or the MNW model otherwise. This subsection demonstrates how the conclusions found in the two-link network are extended to the n independent links/ routes network shown in Fig. 5.

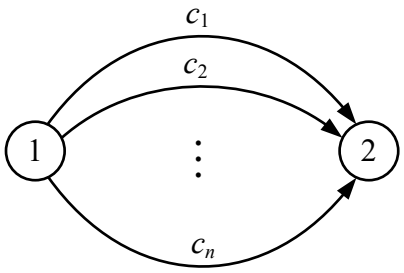

Fig. 5. Network II: Single O-D pair's network with n independent links.

For the MNL model, the partial derivative of the total travel cost C^L with respect to c_1 in Network II are as follows:

$$\frac{\partial C^L}{\partial c_1} = Q\frac{\sum_{i=1}^{n}\exp(-\theta(c_i-c_1))(1+\theta(c_i-c_1))}{\exp(2\theta c_1)\left(\sum_{i=1}^{n}\exp(-\theta c_i)\right)^2}. \tag{21}$$

For the MNL, whether the paradox occurs in a single O-D pair's network with n independent links is determined by absolute cost differences. Denote $a_i = c_i - c_1$ to be the absolute cost difference between route i and route 1. Let $[0, a_2^*, \cdots a_n^*]^T$ represents a feasible basic solution of $\partial C^L/\partial c_1 = 0$ in the real number range without considering link travel costs' positive constraints, and then the general solutions considering link travel costs' positive constraints can be written as:

$$\begin{bmatrix} c_1 \\ c_2 \\ \vdots \\ c_n \end{bmatrix} = \begin{bmatrix} 0 \\ a_2^* \\ \vdots \\ a_n^* \end{bmatrix} - \begin{bmatrix} \min\{0, a_2^*, \cdots a_n^*\} \\ \min\{0, a_2^*, \cdots a_n^*\} \\ \vdots \\ \min\{0, a_2^*, \cdots a_n^*\} \end{bmatrix} + k\begin{bmatrix} 1 \\ 1 \\ \vdots \\ 1 \end{bmatrix};\ \ k \in R^+. \tag{22}$$

To intuitively describe the characteristics of the paradox boundary, the paradox boundary of the MNL model for $n = 3$ and $\theta = 0.1$ case was numerically solved and illustrated in Fig. 6 for a deeper understanding to Eq.(22).

In Fig. 6, it can be seen that the paradox boundary of the MNL model is a curved surface spanned by a series of vectors, each of the vectors passes a specific point $[0, a_2^*, \cdots a_n^*]^T$ and with the direction $[1, \cdots 1]_{1\times n}^T$ (satisfies Eq.(22)). The upper side of the surface is the paradox area, the lower side is the no paradox area. Although Fig. 6 is only a case for $n = 3$, the basic characteristics are illustrated for general cases.

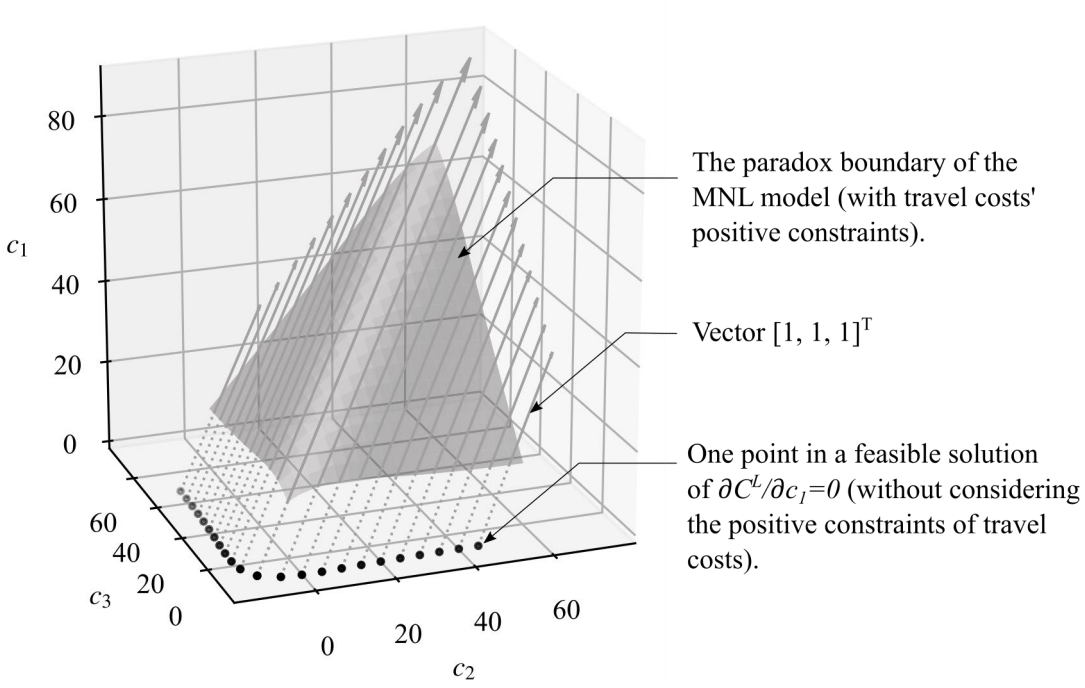

Fig. 6. Paradox boundary of the MNL model in one O-D three links network when $\theta = 0.1$.

Similarly, for the MNW model, the partial derivative of the total travel cost C^W with respect to c_1 in Network II are as follows:

$$\frac{\partial C^W}{\partial c_1} = Q\frac{\sum_{i=1}^{n}\left(\frac{c_i}{c_1}\right)^{-\beta}\left(\beta\left(\frac{c_i}{c_1}\right)+1-\beta\right)}{c_1^{2\beta}\left(\sum_{i=1}^{n} c_i^{-\beta}\right)^2}. \tag{23}$$

For the MNW model, whether the paradox occurs in a single O-D pair's network with n independent links is determined by the relative cost differences. Denote $r_i = c_i/c_1$ to be the relative cost difference between route i and route 1. Let $[1, r_2^*, \cdots r_n^*]^T$ represents a feasible basic positive solution of $\partial C^W/\partial c_1 = 0$, then the general solutions based on this feasible basic positive solution can be written as:

$$\begin{bmatrix} c_1 \\ c_2 \\ \vdots \\ c_n \end{bmatrix} = k\begin{bmatrix} 1 \\ r_2^* \\ \vdots \\ r_n^* \end{bmatrix};\ \ k \in R^+. \tag{24}$$

Also, the paradox boundary of the MNW model when $n = 3$ and $\beta = 3$ was numerically solved and illustrated in Fig. 7. From Fig. 7, it is clear that the paradox boundary of the MNW model is a curved surface spanned by a series of vectors, each of the vector starts in origin and with the direction $[1, r_2^*, \cdots r_n^*]^T$ (satisfies Eq.(24)). The upper side of the surface is the paradox area, and the lower side is the no paradox area.

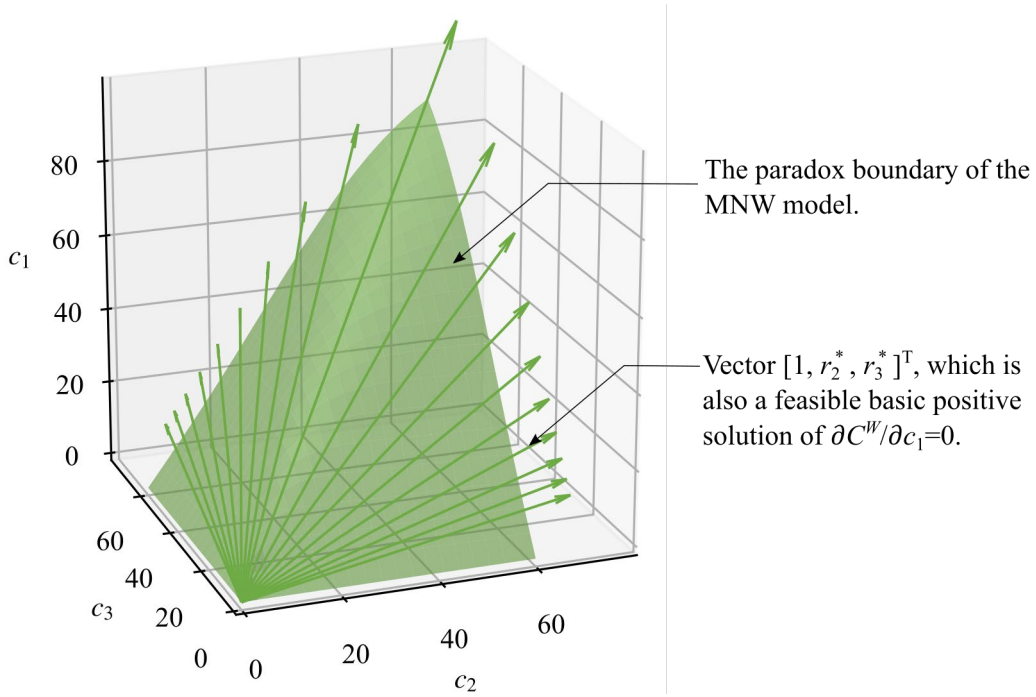

Fig. 7. Paradox boundary of the MNW model in one O-D three links network when $\beta = 3$.

For the MH model, the partial derivative of the total travel cost C^{MH} with respect to c_1 in Network II are:

$$\frac{\partial C^{MH}}{\partial c_1} = Q\frac{\sum_{i=1}^{n} e^{-\theta(c_i-c_1)}\left(\frac{c_i}{c_1}\right)^{-\beta}\left(\beta\left(\frac{c_i}{c_1}\right)+\theta(c_i-c_1)+1-\beta\right)}{e^{2\theta c_1}c_1^{2\beta}\left(\sum_{i=1}^{n} e^{-\theta c_i}c_i^{-\beta}\right)^2}. \tag{25}$$

The paradox boundary of the MH model cannot be decided only by the relative/absolute cost differences. Thus the paradox boundary are numerical solved, and the paradoxical features of the MH model can be easily observed when putting three models together as shown in Fig. 8. It shows that the relationships among the three models in $n = 3$ case are similar to the $n = 2$ case (compare with Fig. 3).

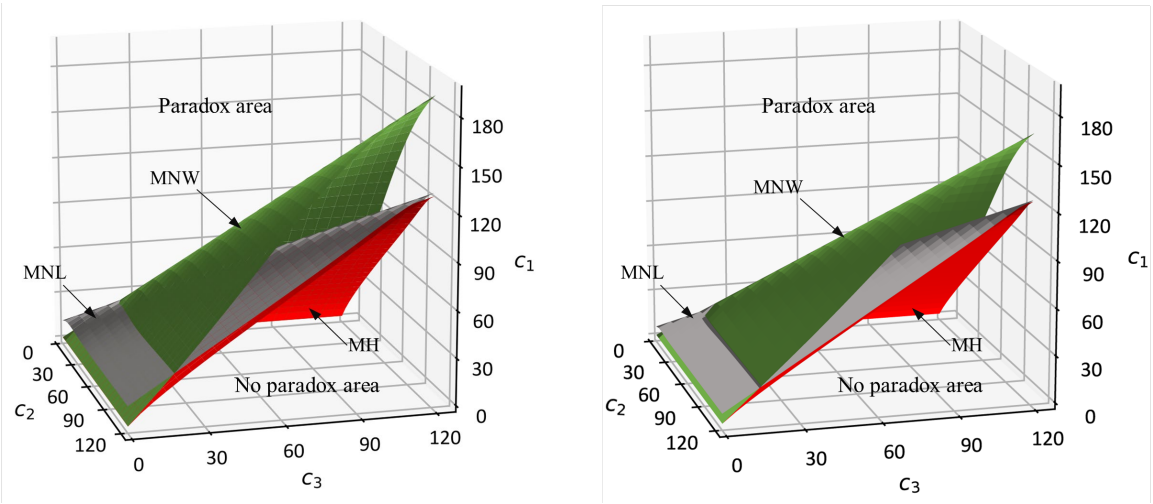

(a) When $\theta = 0.1$, $\beta = 3$, and $\lambda = 0.5$. (b) $\theta = 0.2$, $\beta = 4$, and $\lambda = 0.5$.

Fig. 8. Paradox boundaries of the three models when $n = 3$.

To make the conclusions more convincing, we use two set of different parameters in Fig. 8. From Fig. 8, when the MH model has the same θ and β as the MNL model and the MNW model, the following observations can be found, which correspond to the three observations of Fig. 3:

1. When c_2 or c_3 approximates to zero, the paradox boundary of the MH model approximates to the paradox boundary of the MNW model.

2. When both c_2 and c_3 approximates to a large positive value, the paradox boundary of the MH model approximates to the paradox boundary of the MNL model.

3. The MH model has the biggest paradox area, and its paradox boundary is on the lower side of which of the MNL and MNW models.

4. The above three observations are consistent in Fig 8 (a) and (b).

A qualitative conclusion can be seen from the discussions and the figures above. The no paradox area lies in where the cost of the marginally improved link c_1 is relatively small compared with other links. When the marginal improved link is very poor compared with other links, $\partial C/\partial c_1 < 0$ is always true and the overall travel cost will increase, although the increase is very slight when c_1 becomes exceedingly large.

In the real world, however, improving a very poor link may not always increase the total travel cost. Firstly, extremely long routes may never be chosen (at least not as sensitive as the theory) even if the existence of the theoretical possibility. Travelers find their routes within a route set with relatively short and close travel costs. Secondly, congestions are common on the real roads, which make networks in reality far more complicated than the simple cases of this paper. Finally, if the improvement is significant, which decreases the cost of the inferior link from paradox area to no paradox area (steps over the peak with highest total travel cost), the "marginal improved paradox" may be avoided.

3.3. Overlapping effect

This section discusses the stochastic assignment paradox when an overlapping link is marginally improved.

Considering a single O-D network with n routes, there is a small improvement in an overlapping link shared by m $(m \le n)$ different routes. In convenience, travel costs of the routes with the overlapping link are set to $c_1 \cdots c_m$, the remaining routes' costs are set to $c_{m+1} \cdots c_n$, the cost of the overlapping link is x $(x < \min(c_1 \cdots c_m))$. Then, the marginal effect of a small improvement in the overlapping link can be derived as follows:

$$\frac{\partial C}{\partial x} = \sum_{i=1}^{m} \frac{\partial C}{\partial c_i}\frac{\partial c_i}{\partial x} = \sum_{i=1}^{m} \frac{\partial C}{\partial c_i}, \tag{26}$$

where, C is the total travel cost. Eq. (26) shows that improving an overlapping link is equivalent to improve those m routes simultaneously in a route-independent network.

We use a network shown in Fig. 9 with $n = 3$ and $m = 2$ to further illustrate the stochastic assignment paradox when improving an overlapping link. In the example network, routes are numbered 1, 2, 3 from top to bottom with travel cost of c_1, c_2 and c_3, the name and the cost of each link are shown in the figure. We investigate the stochastic paradox when route 1 is improved. When the improvement occurs in link b, the

effect is the same as the three independent links' case, we compare it with the case when link a gets improved (improving an overlapping link).

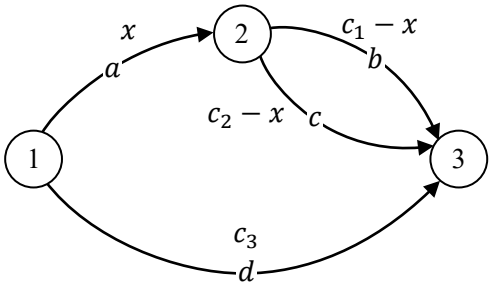

Fig. 9. Network III: Single O-D pair's network with one overlapping link.

The MNL model is used as an example to show the changes of paradox boundary (area) when the improvement on the non-overlapping link moved to the overlapping link. For easy comparison, c_3 is fixed to 30, let $\theta = 0.1$, and $\beta = 3$, results are shown in Fig. 10 (a). The solid line in Fig. 10 (a) is the paradox boundary when the non-overlapping link b is improved, it is obtained by solving $\partial C^L/\partial c_1 = 0$ using Eq.(21). Readers may find this line can also be deemed as a slice of the MNL model's boundary surface in Fig. 8 when $c_3 = 30$. We use the dash line to represent the paradox boundary when the overlapping link a gets a marginal decrease, it can be gained by numerically solving $\partial C^L/\partial x = 0$.

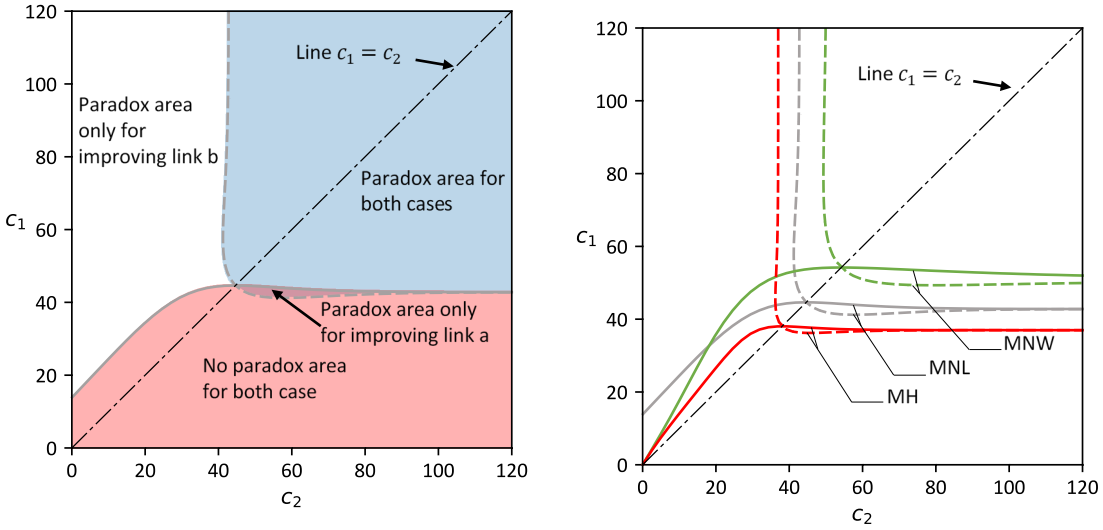

(a) The MNL model (b) All the three models

Fig. 10. Comparison of the paradox boundaries when link a or link b get improved ($c_3 = 30$, solid line for improving link b, dash line for improving link a).

Main observations of Fig. 10 (a) are as follows:

1. The two boundary lines intersect at a point where $c_1 = c_2$. It is easy to understand since when $c_1 \sim c_m$ are equal, $\frac{\partial C}{\partial c_1} \sim \frac{\partial C}{\partial c_m}$ equal to zeros, then $\frac{\partial C}{\partial x} = \sum_{i=1}^{m} \frac{\partial C}{\partial c_i} = 0$.

2. When $c_1 > c_2$, there is an area where paradox only takes place for improving link b. After the

improvement shifted to link a, not only route 1, but also route 2 whose cost is smaller than route 1 is improved which leads to the paradox disappear. It means that the benefit from improving route 2 offsets the paradox generated by improving route 1.

3. When $c_1 < c_2$, there is an area where initially no paradox for improving link b. After the improvement shifted to link a, not only route 1, but also route 2 which has a larger cost gets improved which lead to the paradox occur. It means the benefit from improving route 1 offset the paradox generated by improving route 2.

4. With c_2 getting larger, the paradox boundary for improving link a approaches to the boundary for improving link b, and the paradox area only for improving link a narrows down. It can be explained by the paradox effect is very slight when the cost of the improved route becomes very big compared with other routes, therefore when c_2 gets very big, the paradox boundary is dominated by c_1 and the curves of the two cases become very close.

A small improvement in a superior route tends to save the total travel cost, whereas marginally improving an inferior route is more likely to bring a paradox, the final effect of improving an overlapping link is a combination of the effects of improving the routes that share the overlapping link. Fig. 10 (b) compares the paradox boundaries when improving an overlapping or non-overlapping link for all the three models; observations are the same as the MNL model.

Next, we use Fig. 11 to illustrate the relationships between the paradox boundaries of the three models when improving an overlapping link.

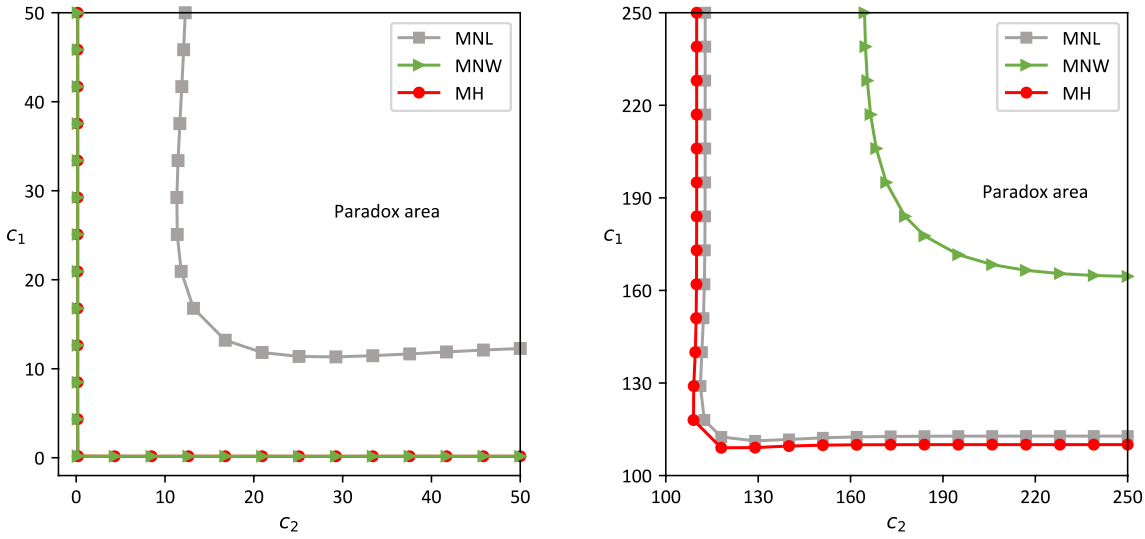

(a) $c_3 = 0.1$ (b) $c_3 = 100$

Fig. 11. Paradox boundaries of the three models when improving the overlapping link a when $\theta = 0.1$ and $\beta = 3$

Fig. 11 (a) is used to represent the case when the cost of the non-improved route approaches to zeros. We can find that the paradox boundary of the MH model almost overlaps with the boundary curve of the MNW model. Besides, for the paradox boundaries of the MNW and MH models, at least one of the improved routes' costs approach to zeros. Fig. 11 (b) shows when the travel cost of the non-improved route is relatively large, the paradox boundary of the MH model is dominated by the MNL model. Also, the MH model has the biggest

paradox area in both cases. All these observations are consistent with previous sections when improving a non-overlapping link. Therefore we can infer that previous conclusions are still valid when n and m become bigger.

Finally, a brief discussion for the multi-O-D network. Based on the premise that road costs are flow independent, the travel cost of each O-D pair can be calculated separately without co-relationship with other O-D pairs. Therefore, for a network with N O-D pairs, when marginally improving a link with cost x, the partial derivative of the total travel cost C with respect to x can be derived as follows:

$$\frac{\partial C}{\partial x} = \frac{\partial \sum_{i=1}^{N} C^i}{\partial x} = \sum_{i=1}^{N} \frac{\partial C^i}{\partial x}, \tag{27}$$

where C^i is the travel cost of O-D pair i. We have discussed the paradox under the single O-D case, Eq. (27) shows whether a paradox occurs in the overall network level is the sum of the paradox effect from each O-D pair.

4. The paradox when using estimated parameters

The preceding sections compare the stochastic traffic paradox boundary of the MH model with the MNL model and the MNW model under the same parameters. However, as discussed in section 3.1.3, parameters of different models are not necessarily the same in practice. This section uses the Multinomial Probit model (MNP) (Daganzo and Sheffi, 1977) to generate simulated route sample data. We will next estimate the parameters for the three route choice models from the sample data to study 1) the relation of the estimated parameters in different models and 2) the stochastic traffic paradox of the three models under the estimated parameters.

4.1. Generate simulated sample data

We use the Sioux-Falls Network (Transportation Networks, 2018), which has been extensively used in transportation literature (e.g., Wang et al., 2019), to carry out the study. We only consider flow-independent case with free-flow travel time; the link IDs are shown in Fig. 12. The route samples are generated through two steps: 1) generating route choice sets and 2) extracting samples from the generated route sets. The MNP model duly addresses the correlations between routes and the heteroscedastic variance; it has been widely applied to generate route set. Therefore, the route samples are generated by a simulation approach using the MNP model.

For a link with cost c_i, the MNP model assumes the perceived cost of the link satisfies Normal distribution $N(c_i, (c_i \times p)^2)$, where p is a factor controls the magnitude of the perceived error. Using the Monte Carlo technique, link costs are randomly generated in each iteration. The shortest route of each iteration will be added into the route choice set. Here we choose $p = 0.2$ and the number of iterations is 1000. For stability, only the routes occur more than 5 (1000×5‰) times are added into route set. Twelve O-D pairs representing various route lengths are selected to generate route sets, they are O-D (1, 20), (1, 18), (13, 2), (13, 7), (2, 23), (4, 22), (4, 19), (12, 21), (5, 18), (14, 20), (10, 19), and (3, 11). On average, 4.1 routes were generated for each O-D pair, the maximum number of routes for an O-D pair was 8. The stochastic user equilibrium performed in the Sioux-Falls network with such route choice set size could achieve a reasonable equilibrium level.

When choosing a sample from a route choice set, we use the MNP model to randomly generate link costs, the

chosen sample is the shortest route among the route choice set. In each sampling, we take 50 samples from each route choice set and collectively obtain 50×12=600 route samples.

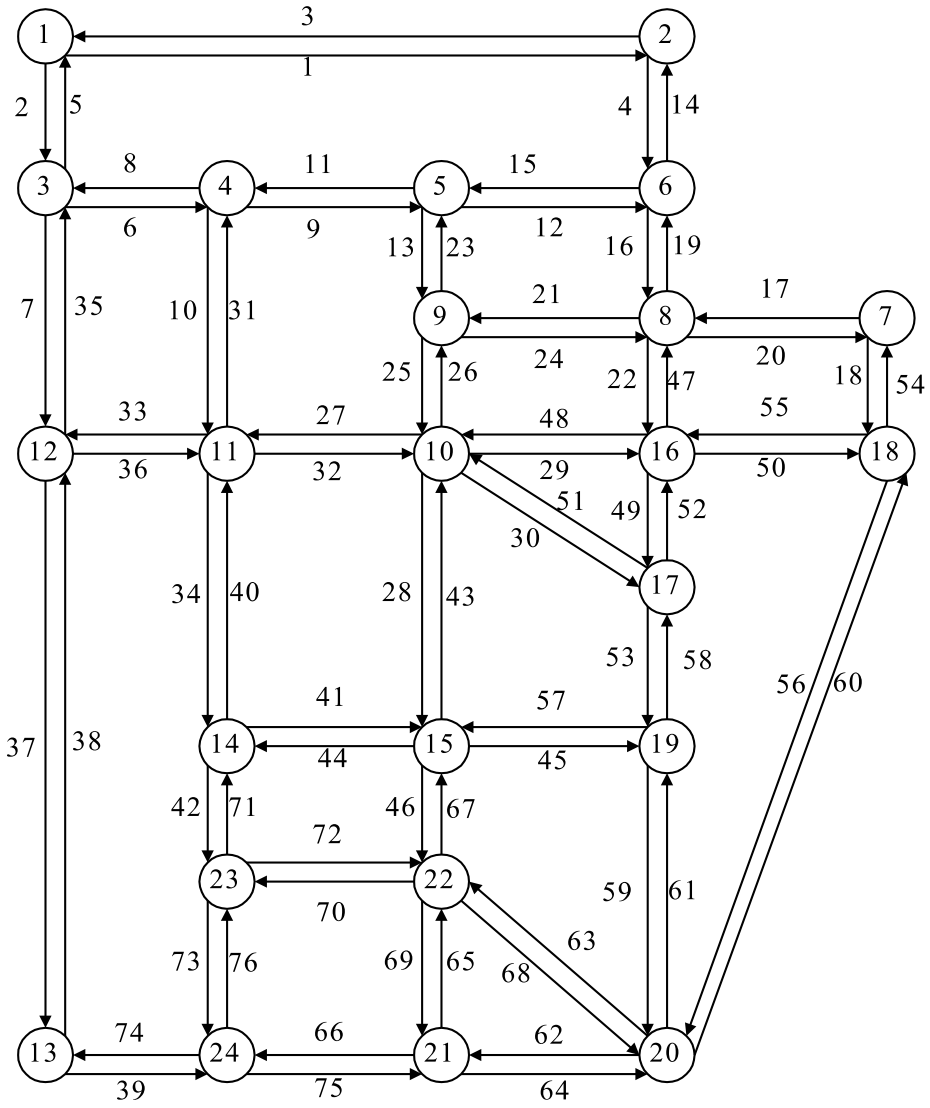

Fig. 12 The Sioux-Falls Network

4.2. Relation of the estimated parameters

Models' parameters are obtained by the Maximum Likelihood Estimate (MLE). Repeat the sampling and the parameter estimation process for 1000 times, 1000 groups of parameters are obtained.

The average log-likelihood of the MNL model, the MNW model, and the MH model in the 1000 groups of estimations are – 473.59, – 483.02, and – 472.56, respectively. To compare the fitness of the MH model with the other two models, the relative differences between the log-likelihood of the MH model and the other two models are calculated (e.g., $(\log\mathcal{L}_{\mathrm{MH}} - \log\mathcal{L}_{\mathrm{MNL}})/|\log\mathcal{L}_{\mathrm{MNL}}|$ is the relative difference between the MH model and the MNL model). The estimation results are shown in Fig. 13. It can be found that the MH model has larger log-likelihood than the other two models and fits the samples better. This is understandable, because the MNL model and the MNW model are special cases of the MH model, the estimation of the MH model will

be no worse than the other two models.

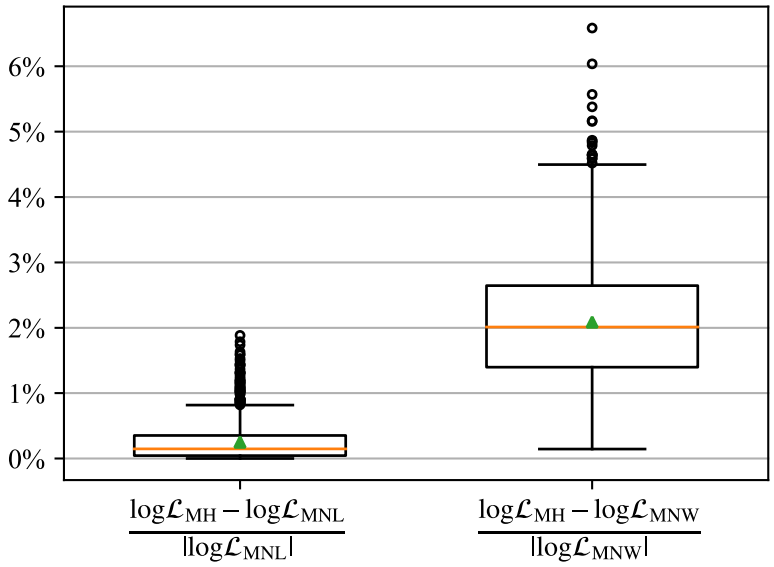

Fig. 13 The comparison of the log-likelihood of the three models

For the MH model, the 1000 groups of parameters are visualized in a scatter plot. Combining with the histograms, the relations between the estimated parameters of the three models are clearly shown in Fig. 14. From the histograms, it can be found the estimation of each parameter nearly satisfies normal distribution. Under the same samples, the estimated θ in the MH model has a smaller mean value and a larger standard deviation compared with the MNL model; the estimated β in the MH model has a smaller mean value and a larger standard deviation compared with the MH model.

Fig. 14 shows the estimation of β has some negative values for the MH model. As discussed in section 2, θ and β should be non-negative to guarantee the utility term to be a non-increasing function with regard to all positive real route costs. However, the estimated parameters only guarantee Eq. (3) to hold for all samples (rather than all positive real values), which leads to a few negative estimations. Note that the mean of the estimated β for the MH model is still positive.

When the estimation of β in the MH model closes to zero, the corresponding estimated θ is around the mean value of the estimated θ of the MNL model. Because the MH model is equivalent to the MNL model when $\beta = 0$. When the estimation of θ in the MH model closes to zero, the corresponding estimated β is around the mean value of the estimated β of the MNW model. Because the MH model is equivalent to the MNW model when $\theta = 0$.

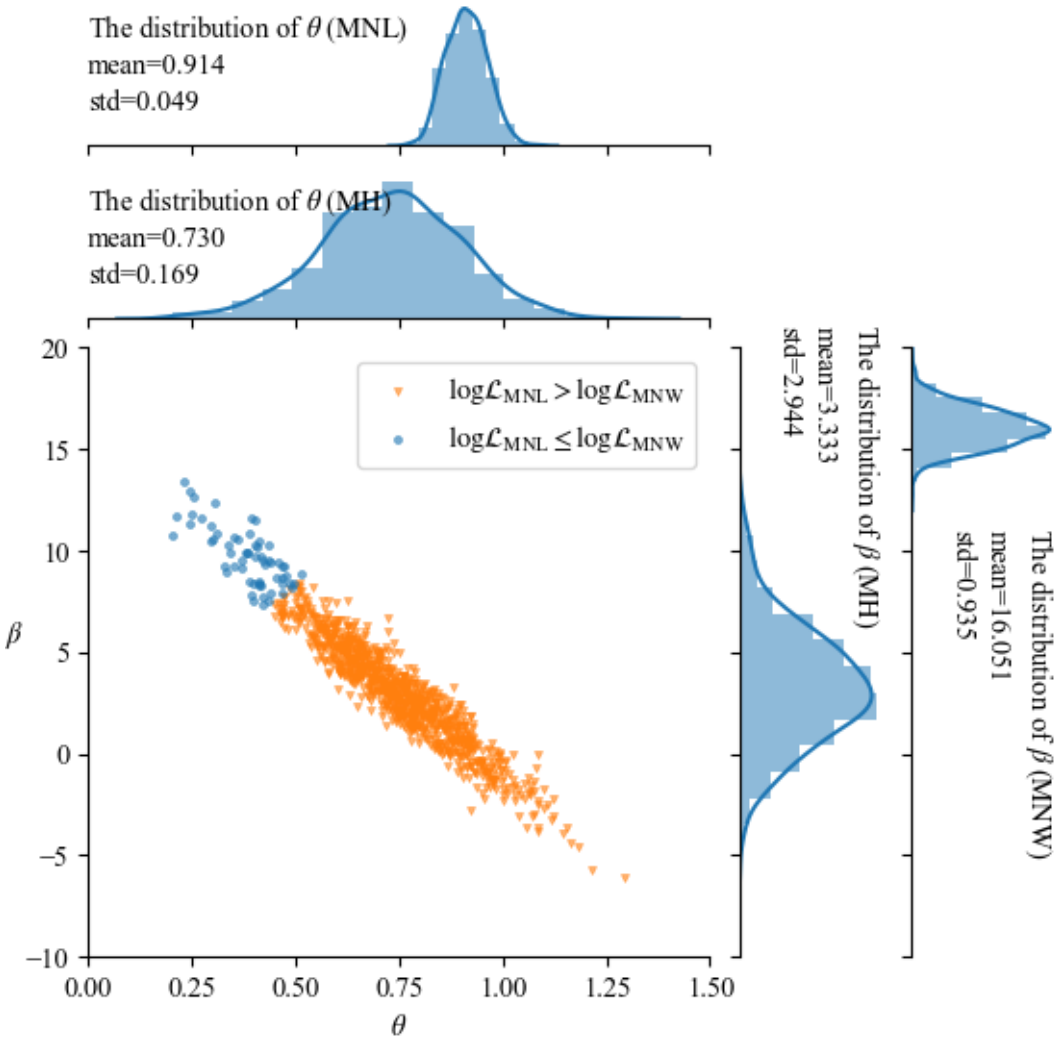

Fig. 14 The relations between the estimated parameters in the three model

The orange triangle represents when the estimation of the MNL model is better than the estimation of the MNW model (i.e., the log-likelihood function of the MNL model $\log\mathcal{L}_{\mathrm{MNL}}$ is larger than which of the MNW model $\log\mathcal{L}_{\mathrm{MNW}}$), and the blue dot represents when the MNW model has a better estimation compared with the MNL model. It can be found that when the MNL model has a better estimation, the estimation of the MH model tends to be determined by the MNL model (i.e., a bigger θ and a smaller β). Accordingly, the MNW model part dominates the MH model (i.e., a smaller θ and a bigger β) when the MNW model has a better estimation. By leaning to the model with better estimation, the MH model has a better (at least equivalent) estimation than the original models.

4.3. Identifying paradox links using estimated parameters

When marginally reducing the travel cost of a link a increases the total travel costs of an O-D pair O, we refer to the link a as a paradox link for this O-D pair. The objective of this section is to compare the differences in identifying paradox links using the estimated parameters of different models. Recall that section 3.1 to section 3.3 have emphasized the difference of the paradoxical feature of the three models between 0^+ and $+\infty$ link costs, this section correspondingly inspects a short O-D pair (10, 19) and a long O-D pair (1, 20).

If a model indicates that a link is a paradox link, we call it a "positive result" of a paradox link. For the short O-D pair, the number of positive results for links in O-D (10, 19) under 1000 groups of estimated parameters is shown in Tab. 1. For the long O-D pair, the results are shown in Tab. 2. Note that the two tables only include links that belong to the route choice sets of these O-D pairs. The "All" column in the tables means the number of links that are paradox links in all three models.

Tab. 1 The number of positive results for links in O-D (10, 19)
under 1000 groups of estimated parameters

link ID	MNL	MNW	MH	All
45	0	1000	57	0
49	0	0	0	0
53	0	0	0	0
28	0	1000	57	0
29	0	0	0	0
30	1000	1000	995	995

Tab. 2 The number of positive results for links in O-D (1,20)
under 1000 groups of estimated parameters

link ID	MNL	MNW	MH	All
1	0	0	0	0
2	1000	557	998	557
4	0	0	0	0
6	1000	977	1000	977
7	1000	342	998	342
9	1000	977	1000	977
12	1000	977	1000	977
16	0	0	0	0
18	0	0	0	0
20	0	0	0	0
22	1000	1000	1000	1000
37	1000	342	998	342
39	1000	342	998	342
49	1000	1000	1000	1000
53	1000	1000	1000	1000
56	0	0	0	0
59	1000	1000	1000	1000
64	946	0	701	0
65	1000	977	1000	977
68	1000	999	1000	999
72	1000	1000	1000	1000
75	1000	33	984	33
76	1000	1000	1000	1000

Although the general results of the three models in Tab. 1 and Tab. 2 are similar, the results for some links show significant inconsistency. There are three main observations:

1. For the short O-D (10, 19), the number of potential paradox links identified by the MNL model is generally less than which of the MNW model and the MH model.

2. For the long O-D (1, 20), links are more likely to be identified as paradox links in the MNL model compared with the other two models.

3. For the MH model, the number of positive results is between the MNL model and the MNW model (with only two exceptions for the link 30 in O-D (10, 19) and the link 64 in O-D (1, 20)).

As discussed in section 3, the paradox boundaries of the MNW model and the MH model ($\beta > 1$) when any of the non-improved route' cost approaches to zero are on the "lower" side of which of the MNL model. Therefore, the MNW model and the MH model have a larger paradox area than the MNL model when routes' costs are small, which corresponds to the first observation. Similarly, the second observation can be explained by the paradox boundary of the MNL model is on the "lower" side (larger paradox area) of which of the MNW model and the MH model when the non-improved routes' costs are very large (ideally, approach to the $+\infty$).

If the MH model uses the same parameter as the MNL model and the MNW model, it is expected that the MH model identifies more paradox links than the other two models for both the long and the short O-D pairs. As discussed in section 3.1.3, only when using smaller β and θ simultaneously in the MH model can the paradox boundary of the MH model be a compromise of the MNL and MNW models. The relations of the estimated parameters in section 4.2 show that the estimated θ and β of the MH model are averagely smaller than which in the MNL model and the MNW model. This results in observation 3, the number of positive results of paradox links in the MH model is generally between the number of the MNL model and the MNW model.

In summary, using the simulated data, the identification of paradox links when using the estimated parameters in the three model shows intrinsic tendencies, which can be explained by the paradoxical features of the three models. Compared with two original models, the MH model fits data the best, and the prediction of paradox links in the MH model is more moderate.

5. Concluding remarks

This paper compared the traffic paradox features of three stochastic route choice models (MNL, MNW, and MH) when an inferior travel alternative is marginally improved under uncongested networks (cost of links are independent of the flow). On the one hand, the relationships between the paradox conditions (paradox boundary) in the three models are studied when the MH model has the same parameters as the MNL and the MNW model. We find consistent paradoxical features for all three typical small networks studied (two links, n independent links, and three routes with an overlapping link): 1) The stochastic assignment paradox of the MH model is dominated by the MNW model when any of the non-improved links approaches to zero, 2) it is controlled by the MNL model when all of the non-improved links approaches to infinity, and 3) the MH model has a larger paradox area than the MNL and MNW models. On the other hand, the stochastic

assignment paradoxes of the three models are also compared when using estimated parameters. The results show that 1) the MH model fits the route samples the best, 2) the MNW tends to identify more links to be paradox links in short O-D pairs, 3) the MNL model tends to identify more links to be paradox links in long O-D pairs, and 4) the identification result of the MH model is a compromise of other two models.

The findings of this work also provide suggestions and caveats to the application of the three models. One should understand the paradoxical feature of the three models when diagnosing the stochastic paradox, and special attention should be paid to extremely long or short O-D pairs. We should aware that the MNW and the MNL model tend to overestimate the stochastic paradox for long and short O-D pairs, respectively. The MH model is a better model in the sense of the fitness to data and the moderateness in paradox detection.

This paper also has some limitations. Firstly, congestion is very common in real networks and assuming flow-independent travel times is too idealistic. Secondly, all the three route choice models of this paper assume that random error terms are independent, none of them can capture overlapping features properly due to this assumption. Therefore, further research should be conducted in the following aspects. Firstly, paradoxical features should be examined under congested road networks using the stochastic user equilibrium (SUE) model (Yao et al., 2019a; Zhou et al., 2014; Yu et al.). Secondly, overlapping effect should be studied under route choice models which consider the correlations between routes, such as Probit model (Daganzo and Sheffi, 1977), C-logit model (Cascetta et al.,1996; Zhou et al., 2012), Nested Logit (NL) model (McFadden, 1978), path-size logit (PSL) model (Chen et al., 2012). Adapting fast path-based algorithms for traffic assignment to these route choice model is also interesting (Chen et al., 2001; Perederieieva et al., 2018; Du et al., 2020). Finally, various route choice models and their paradoxical features should be applied to a broader range of problems, such as network design (Cantarella et al., 2006; Hosseininasab et al., 2018), network evaluation (Han et al., 2008), combined modal split and traffic assignment problem (Xu et al., 2008; Ryu et al., 2017).

Acknowledgments

This research was partially supported by the National Natural Science Foundation of China (71871075, 71501053, 91846301), China Postdoctoral Science Foundation (2015M570297), International Postdoctoral Exchange Fellowship (20160076) of China Postdoctoral Council, Research Grants Council of the Hong Kong Special Administrative Region (15212217), Research Committee of the Hong Kong Polytechnic University (Project No. 1-ZVJV), and CCF-DiDi Big Data Joint Lab.

References

Acemoglu, D., Makhdoumi, A., Malekian, A., & Ozdaglar, A. (2018). Informational Braess' paradox: the effect of information on traffic congestion. Operations Research, 66(4), 893-917.

Akamatsu, T. (2000). A dynamic traffic equilibrium assignment paradox. Transportation Research Part B: Methodological, 34(6), 515-531.

Arnott, R., De Palma, A., & Lindsey, R. (1993). Properties of dynamic traffic equilibrium involving bottlenecks, including a paradox and metering. Transportation Science, 27(2), 148-160.

Bagloee, S. A., Sarvi, M., Wolshon, B., & Dixit, V. (2017). Identifying critical disruption scenarios and a global robustness index tailored to real life road networks. Transportation Research Part E: Logistics and Transportation Review, 98, 60-81.

Braess, D. (1968). Über ein Paradoxon aus der Verkehrsplanung. Unternehmensforschung, 12(1), 258-268.

Braess, D., Nagurney, A., & Wakolbinger, T. (2005). On a paradox of traffic planning. Transportation Science, 39(4), 446-450.

Cantarella, G. E., Pavone, G., & Vitetta, A. (2006). Heuristics for urban road network design: lane layout and signal settings. European Journal of Operational Research, 175(3), 1682-1695.

Cascetta, E., Nuzzolo, A., Russo, F., & Vitetta, A. (1996). A modified logit route choice model overcoming path overlapping problems. Specification and some calibration results for interurban networks. In Transportation and Traffic Theory. Proceedings of the 13th International Symposium on Transportation and Traffic Theory, Lyon, France.

Castillo, E., Menéndez, J. M., Jiménez, P., & Rivas, A. (2008). Closed form expressions for choice probabilities in the Weibull case. Transportation Research Part B: Methodological, 42(4), 373-380.

Chen, A., Lo, H., & Yang, H. (2001). A self-adaptive projection and contraction algorithm for the traffic assignment problem with path-specific costs. European Journal of Operational Research, 135(1), 27–41.

Chen, A., Pravinvongvuth, S., Xu, X., Ryu, S., & Chootinan, P. (2012). Examining the scaling effect and overlapping problem in logit-based stochastic user equilibrium models. Transportation Research Part A: Policy and Practice, 46(8), 1343-1358.

Daganzo, C. F., & Sheffi, Y. (1977). On stochastic models of traffic assignment. Transportation Science, 11(3), 253-274.

Di, X., He, X., Guo, X., & Liu, H. X. (2014). Braess paradox under the boundedly rational user equilibria. Transportation Research Part B: Methodological, 67, 86-108.

Downs, A. (1962). The law of peak-hour expressway congestion. Traffic Quarterly, 16(3), 393-409.

Du, M., Tan, H., Chen, A. (2020) A faster path-based algorithm with Barzilai-Borwein step size for solving stochastic traffic equilibrium models. European Journal of Operational Research.

Fisk, C. (1979). More paradoxes in the equilibrium assignment problem. Transportation Research Part B: Methodological, 13(4), 305-309.

Hallefjord, A., Jørnsten, K., & Storøy, S. (1994). Traffic equilibrium paradoxes when travel demand is elastic. Asia-Pacific Journal of Operations Research 11 (1), 41-50.

Han, D., Lo, H. K., Sun, J., & Yang, H. (2008). The toll effect on price of anarchy when costs are nonlinear and asymmetric. European Journal of Operational Research, 186(1), 300-316.

Henn, V., & Ottomanelli, M. (2006). Handling uncertainty in route choice models: From probabilistic to possibilistic approaches. European Journal of Operational Research, 175(3), 1526-1538.

Hosseininasab, S. M., Shetab-Boushehri, S. N., Hejazi, S. R., & Karimi, H. (2018). A multi-objective integrated model for selecting, scheduling, and budgeting road construction projects. European Journal of Operational Research, 271(1), 262-277.

Kitahara, Y., & Hayakawa, T. (2019). Analysis of Dynamic Traffic Demand on a Paradoxical Phenomenon and Reachability with Input Constraints. In 2019 SICE International Symposium on Control Systems (SICE ISCS) (pp. 65-71). IEEE.

Kitthamkesorn, S., & Chen, A. (2014). Unconstrained weibit stochastic user equilibrium model with extensions. Transportation Research Part B: Methodological, 59, 1-21.

Lin, W. H., & Lo, H. K. (2009). Investigating Braess' paradox with time-dependent queues. Transportation Science, 43(1), 117-126.

Liu, P., Xu, X., Chen, A., Yang, C., & Xiao, L. (2017). A select link analysis method based on logit–weibit hybrid model. Journal of Modern Transportation, 25(4), 205-217.

Ma, C., Cai, Q., Alam, S., Sridhar, B., & Duong, V. N. (2019). Airway network management using Braess's Paradox. Transportation Research Part C: Emerging Technologies, 105, 565-579.

Ma, J., Li, D., Cheng, L., Lou, X., Sun, C., & Tang, W. (2018). Link restriction: Methods of testing and avoiding braess paradox in networks considering traffic demands. Journal of Transportation Engineering, Part A: Systems, 144(2).

McFadden, D. (1978). Modeling the choice of residential location. Transportation Research Record, (673).

Nagurney, A. (2000). Congested urban transportation networks and emission paradoxes. Transportation Research Part D: Transport and Environment, 5(2), 145-151.

Perederieieva, O., Raith, A., & Schmidt, M. (2018). Non-additive shortest path in the context of traffic assignment. European Journal of Operational Research, 268, 325-338.

Prashker, J. N., & Bekhor, S. (2000). Some observations on stochastic user equilibrium and system optimum of traffic assignment. Transportation Research Part B: Methodological, 34(4), 277-291.

Ryu, S., Chen, A., & Choi, K. (2017). Solving the combined modal split and traffic assignment problem with two types of transit impedance function. European Journal of Operational Research, 257(3), 870–880.

Sheffi, Y. (1985). Urban Transportation Networks. Prentice-Hall, Englewood Cliffs, NJ.

Sheffi, Y., & Daganzo, C. F. (1978). Another "paradox" of traffic flow. Transportation Research, 12(1), 43-46.

Steinberg, R., & Zangwill, W. I. (1983). The prevalence of Braess' paradox. Transportation Science, 17(3), 301-318.

Sun, L., Liu, L., Xu, Z., Jie, Y., Wei, D., & Wang, P. (2015). Locating inefficient links in a large-scale transportation network. Physica A: Statistical Mechanics and its Applications, 419, 537-545.

Szeto, W. Y. (2011). Cooperative game approaches to measuring network reliability considering paradoxes. Transportation Research Part C: Emerging Technologies, 19(2), 229-241.

Szeto, W. Y., & Jiang, Y. (2014). Transit assignment: Approach-based formulation, extragradient method, and paradox. Transportation Research Part B: Methodological, 62, 51-76.

Szeto, W. Y., Li, X., & O'Mahony, M. (2008). Simultaneous Occurrence of the Braess and Emission Paradoxes. Proceedings of the 6th International Conference on Traffic and Transportation Studies, 625-634.

Thomson, J.M. (1977). Great Cities and Their Traffic. Victor Gollancz, London.

Transportation Networks for Research Core Team. Transportation Networks for Research. https://github.com/bstabler/TransportationNetworks. Accessed May 16, 2018.

Wang, G., Gao, Z., & Xu, M. (2019). Integrating link-based discrete credit charging scheme into discrete network design problem. European Journal of Operational Research, 272(1), 176-187.

Wang, W. W., Wang, D. Z., Zhang, F., Sun, H., Zhang, W., & Wu, J. (2017). Overcoming the Downs-Thomson Paradox by transit subsidy policies. Transportation Research Part A: Policy and Practice, 95, 126-147.

Wang, Y., & Szeto, W. Y. (2017). Excessive noise paradoxes in urban transportation networks. Transportmetrica A: Transport Science, 13(3), 195-221.

Wardrop, J. G. (1952). Some Theoretical Aspects of Road Traffic Research. Proceedings of the Institution of Civil Engineers 1 (3), 325-362.

Xu, M., Chen, A., & Gao, Z. (2008). An improved origin-based algorithm for solving the combined distribution and assignment problem. European Journal of Operational Research, 188(2), 354–369.

Xu, X., Chen, A., Kitthamkesorn, S., Yang, H., & Lo, H. K. (2015). Modeling absolute and relative cost differences in stochastic user equilibrium problem. Transportation Research Part B: Methodological, 81, 686-703.

Yang, C., & Chen, A. (2009). Sensitivity analysis of the combined travel demand model with applications.

European Journal of Operational Research, 198(3), 909-921.
Yang, H. (1997). Sensitivity analysis for the elastic-demand network equilibrium problem with applications. Transportation Research Part B: Methodological, 31 (1): 55-70.
Yang, H., & Bell, M. G. (1998). A capacity paradox in network design and how to avoid it. Transportation Research Part A: Policy and Practice, 32(7), 539-545.
Yao, J., & Chen, A. (2014). An analysis of logit and weibit route choices in stochastic assignment paradox. Transportation Research Part B: Methodological, 69: 31-49.
Yao, J., Cheng, Z., Dai, J., Chen, A., & An, S. (2019a). Traffic assignment paradox incorporating congestion and stochastic perceived error simultaneously. Transportmetrica A: Transport Science, 15(2), 307-325.
Yao, J., Huang, W., Chen, A., Cheng, Z., An, S., & Xu, G. (2019b). Paradox links can improve system efficiency: An illustration in traffic assignment problem. Transportation Research Part B: Methodological, 129, 35-49.
Yao, J., Shi, F., An, S., & Wang, J. (2015). Evaluation of exclusive bus lanes in a bi-modal degradable road network. Transportation Research Part C: Emerging Technologies, 60, 36-51.
Yu, Q., Fang, D., & Du, W. (2014). Solving the logit-based stochastic user equilibrium problem with elastic demand based on the extended traffic network model. European Journal of Operational Research, 239, 112-118.
Zhang, X., Lam, W. H., & Huang, H. J. (2008). Braess's paradoxes in dynamic traffic assignment with simultaneous departure time and route choices. Transportmetrica, 4(3), 209-225.
Zhao, C., Fu, B., & Wang, T. (2014). Braess paradox and robustness of traffic networks under stochastic user equilibrium. Transportation Research Part E: Logistics and Transportation Review, 61, 135-141.
Zhou, Z., Chen, A., & Wong, S. (2009). Alternative formulations of a combined trip generation, trip distribution, modal split, and trip assignment model. European Journal of Operational Research, 198, 129-138.
Zhou, Z., Chen, A., & Bekhor, S. (2012). C-logit stochastic user equilibrium model: formulations and solution algorithm. Transportmetrica, 8(1), 17-41.
Zhou, B., Li, X., & He, J. (2014). Exploring trust region method for the solution of logit-based stochastic user equilibrium problems. European Journal of Operational Research, 239, 46-57.